

Post-print of the article published in Separation and Purification  
Technologies:

Diffusion Dialysis for the treatment of H<sub>2</sub>SO<sub>4</sub>-CuSO<sub>4</sub> solutions from electroplating plants:  
ions membrane transport characterization and modelling.

A. Ruiz-Aguirre, J. Lopez, R. Gueccia, S. Randazzo, A. Cipollina, J. L. Cortina, G. Micale,  
2021. Separation and Purification Technology 266 (2021) 118215 [https://  
doi.org/10.1016/j.seppur.2020.118215](https://doi.org/10.1016/j.seppur.2020.118215)

# Diffusion Dialysis for the treatment of H<sub>2</sub>SO<sub>4</sub>-CuSO<sub>4</sub> solutions from electroplating plants: ions membrane transport characterization and modelling.

*A. Ruiz-Aguirre<sup>a\*1</sup>, J. Lopez<sup>b, c</sup>, R. Gueccia<sup>d</sup>, S. Randazzo<sup>d\*</sup>, A. Cipollina<sup>d</sup>, J. L. Cortina<sup>b, c, e</sup>,  
G. Micale<sup>d</sup>*

<sup>a</sup> CIEMAT – Plataforma Solar de Almería, Ctra. De Senés s/n, 04200 Tabernas, Almería, Spain

<sup>b</sup> Chemical Engineering Department, UPC-BarcelonaTECH, C/Eduard Maristany, 10-14 (Campus Diagonal-Besòs), 08930 Barcelona, Spain.

<sup>c</sup> Barcelona Research Center for Multiscale Science and Engineering, C/Eduard Maristany, 10-14 (Campus Diagonal-Besòs), 08930 Barcelona, Spain.

<sup>d</sup> Dipartimento di Ingegneria, Università di Palermo (UNIPA)-viale delle Scienze Ed. 6, 90128 Palermo, Italy.

<sup>e</sup>Water Technology Center (CETaqua), Carretera d'Esplugues 75, 08940 Cornellà de Llobregat, Spain.

*\*Corresponding Author at CIEMAT – Plataforma Solar de Almería, Ctra. De Senés s/n, 04200 Tabernas, Almería, Spain  
E-mail addresses: alba.ruiz@psa.es (A. Ruiz-Aguirre).*

*\*Corresponding Author at Dipartimento di Ingegneria, Università di Palermo (UNIPA)-viale delle Scienze Ed. 6, 90128  
Palermo, Italy. E-mail addresses: serena.randazzo@unipa.it (S. Randazzo).*

## **Abstract**

Diffusion dialysis (DD) is proposed to separate and recover mineral acids and transition metals from electroplating industry process waters promoting a circular approach of resources recovery. In this work, a DD module with two anionic membranes (Fumasep FAD and Neosepta AFN) are used for the separation of H<sub>2</sub>SO<sub>4</sub> from Cu<sup>2+</sup> containing solutions. The membrane performances with sole H<sub>2</sub>SO<sub>4</sub> solutions (0.2-2 M) and sole CuSO<sub>4</sub> solutions (0.8-1.1 M Cu<sup>2+</sup>) and with mixtures of H<sub>2</sub>SO<sub>4</sub> (0.6 M) and CuSO<sub>4</sub> (0.2-1.1 M Cu<sup>2+</sup>) as feed are studied. H<sub>2</sub>SO<sub>4</sub> recovery efficiency decreases as the concentration of acid increases. For H<sub>2</sub>SO<sub>4</sub> solutions, the water drag flux from the retentate to the diffusate prevails against the osmotic flux for all concentrations investigated. Conversely, the presence of CuSO<sub>4</sub> in solution enhanced the osmotic flux and slightly negatively affected the acid

recovery. The osmotic flux is higher for Fumasep FAD. A distributed parameter model consisting of a set of spatial differential equations for the DD channels and a dynamic section including time-dependent differential equations for batch operations is constructed and then validated using experimental results.

**Keywords:** Copper electroplating; Sulphuric acid recovery; Brine valorization; Circular economy; Industrial wastewater treatment; Diffusion dialysis.

## 1. Introduction

Metallic coatings are commonly used to protect other metals from corrosion and to give to materials enhanced properties, or simply for decorative purposes. Electrolytic deposition is one of the most used technologies. Electroplating industrial effluents contains strong acids such as nitric-hydrofluoric acids mixtures, hydrochloric acid and sulphuric acid and transition metals ions ( $\text{Cu}^{2+}$ ,  $\text{Zn}^{2+}$ ,  $\text{Fe}^{2+}$ ) [1, 2]. Therefore, a treatment of these waste streams is necessary before their discharge or reuse. During decades, solutions were treated with lime to neutralize the presence of strong acids and metal ions and the sludge was disposed in landfill. The increasingly stringent environmental regulations with regard to the disposal of metal containing sludge and the growing attention to concepts of reuse/recycling and circularity are promoting the development of near-zero discharge and the promotion of resource recovery also in these industrial applications [3].

Sustainable treatment of the generated waste acid streams should include the recovery of both valuable metals, as zinc and copper, and acid, which are washed out from the concentrated zinc galvanizing and copper electroplating baths.

To achieve this goal a membrane technology called Diffusion Dialysis (DD) has been proposed in the last years [4]. DD is a membrane separation process in which the driving force is the difference of concentration across the membrane. Membranes for DD are ion-exchange membranes (IEM) and these are usually classified by their function of separation media as cation-exchange membranes (CEM), which contain negative fixed charges and have a selective permeability for cations, and as

anion-exchange membranes (AEM), which contain positive fixed charges and have a selective permeability for anions [4]. AEMs have brought much attention for acid recovery with DD process as their positive fixed charges promote the transport of the strong acids in ionized form (e.g.  $\text{HSO}_4^-$ ,  $\text{Cl}^-$ ,  $\text{NO}_3^-$ ) [5], through the easiest transport of the anions and the easy diffusion of the very small  $\text{H}^+$  ions. The majority of AEMs are usually synthesized from polymers as polysulfone (PSU), polystyrene (PS), and brominated poly (2,6-dimethyl 1,4-phenylene oxide) (BPPO) [6]. Some commercially available AEMs have been evaluated in DD process to recover sulphuric acid, such as the Selemion [7, 8], Neosepta [9, 10], DF-120B [11, 12] and Fumasep FAD [13]. Palatý and Záková evaluated theoretically and experimentally the transport of  $\text{H}_2\text{SO}_4$  through a Neosepta AFN membrane using a two compartment batch cell stirred continuously basing on Fick's law [9, 14-16]. The values of the permeability for the dissociated ions were  $4.82 \cdot 10^{-6}$  m/s and  $3.73 \cdot 10^{-6}$  m/s for  $\text{HSO}_4^-$  and  $\text{SO}_4^{2-}$  respectively while for the non-dissociated specie was  $4.60 \cdot 10^{-6}$  m/s. As mentioned before, the transport of  $\text{H}_2\text{SO}_4$  was also studied in other AEMs. For example, Ersoz et al. [17] evaluated the effect of the concentration and the speed of the stirrer using another type of Neosepta AEM (Neosepta AMH) and polyether-sulfone (SB-6407). According to the data shown in the study, the trend of the mass transfer coefficient ( $k_m$ , m/s) and the diffusion coefficient ( $D$ ,  $\text{cm}^2/\text{s}$ ) were practically the same with the variation of the concentration (from 0.05 to 0.5 M) and the rotational speed of the stirrers (from 2 to  $10 \text{ s}^{-1}$ ).

Other studies focused on the influence of the presence of a metal on the transport of the acid through the membrane have been reported. A new pore-filled anion-exchange membranes (PFAEMs) made with porous polymer substrates without and with polypyrrole coating with good affinity to anions was tested using a feed solution composed of  $\text{H}_2\text{SO}_4$  and  $\text{FeCl}_3$ . The performance was higher than that of a commercial Neosepta AFX when a thin layer of polypyrrole was introduced [18]. Luo et al. [19] obtained a value of  $1.6 \cdot 10^{-6}$  m/s for the permeability of a membrane of poly (2,6-dimethyl-1,4-phenylene oxide) (PPO) for  $\text{SO}_4^{2-}$  considering the presence of its corresponding salt of sodium in the feed solution. Moreover, the recovery of  $\text{H}_2\text{SO}_4$  by AEMs has also been studied considering real

solutions as titanium waste liquor [20], waste anodic aluminium oxidation solution containing  $\text{H}_2\text{SO}_4$ ,  $\text{CuSO}_4$ ,  $\text{Al}_2(\text{SO}_4)_3$  [11] and vanadium leaching solution [21]. In the first case, a good recovery of the acid (acid permeability of about  $133.4 \cdot 10^{-4}$  m/h) and selectivity of 73.3 % and 98.4 % for  $\text{H}_2\text{SO}_4$  over  $\text{Fe}^{2+}$  and  $\text{Ti}^{4+}$ , respectively, were obtained modifying a poly (2,6-dimethyl-1,4-phenylene oxide) (PPO) by bromination, chloromethylation and amination. In the second case,  $\text{H}_2\text{SO}_4$  recovery of 85.25 % and a leakage of  $\text{Al}^{3+}$  of about 5% was obtained with a commercial BPPO membrane (DF120). Finally, in the third case, a DF120 membrane was used to separate  $\text{H}_2\text{SO}_4$  (recovery of 84 %) from V, Al and Fe (rejection of 93 %, 92 % and 85 %, respectively). However, the separation of  $\text{H}_2\text{SO}_4$  from its corresponding copper salt has not drawn much attention. It has been studied utilizing mainly Neosepta membranes both in a two compartment batch cell continuously stirred [22, 23] and in a continuous operation mode [24, 25]. A good separation of the acid was reached with Neosepta AFN membrane ( $\text{H}_2\text{SO}_4$  recovery between 65 % and 90 % and  $\text{Cu}^{2+}$  rejection from 70 % and 98 %) [22, 24, 25]. The permeability of Neosepta AFN for the acid was  $3.1 \cdot 10^{-6}$  m/s and for the copper salt  $2.2 \cdot 10^{-7}$  m/s. The presence of the copper salt decreased the recovery of  $\text{H}_2\text{SO}_4$  (coefficient that represents the influence of the copper salt on the passage of  $\text{H}_2\text{SO}_4$  through the membrane ( $P_{\text{H}_2\text{SO}_4-\text{CuSO}_4}$ ) equal to  $-3.142 \cdot 10^{-9}$  m/s) while the presence of the acid favoured the rejection of the metal ( $P_{\text{CuSO}_4-\text{H}_2\text{SO}_4} = -6.494 \cdot 10^{-7}$  m/s) [25]. Neosepta AMX was used to separate  $\text{H}_2\text{SO}_4$  from different metals ( $\text{Cu}^{2+}$ ,  $\text{Zn}^{2+}$ ,  $\text{Ni}^{2+}$ ,  $\text{Fe}^{3+}$ ,  $\text{Cr}^{3+}$ ,  $\text{Pb}^{2+}$ ) from electroplating sludge [23]. Under optimum conditions, a recovery of  $\text{H}_2\text{SO}_4$  of more than 95 % could be reached. Later, 100 % of  $\text{Cu}^{2+}$  was recovered by cementation. In this context, only two studies were carried out evaluating the permeability of Fumasep FAD. In the first one, the permeability of the membrane for  $\text{H}_2\text{SO}_4$  decreased from  $2.44 \cdot 10^{-5}$  m/s to  $0.87 \cdot 10^{-5}$  m/s when the concentration varied between 0.2 M and 2 M [13]. The second study concerned the reduction of a real pregnant leach solution composed of different acids (HCl and  $\text{H}_2\text{SO}_4$ ) and metals ( $\text{Cu}^{2+}$ ,  $\text{Ni}^{2+}$ ,  $\text{Co}^{2+}$ ,  $\text{Cr}^{3+}$ ,  $\text{Fe}^{3+}$  and  $\text{Al}^{3+}$ ) [26]. The permeability of the membrane for the acid varied from  $0.32 \cdot 10^{-6}$  m/s to  $3.15 \cdot 10^{-6}$  m/s and the maximum rejection of  $\text{Cu}^{2+}$  was 94 %.

In this context, the EU R&D project “Resource recovery from industrial Wastewater by Cutting Edge Membrane technologies” (ReWaCEM)) aims at the development of integrated hybrid technologies for recovery of strong acids and transition metals from four different metal plating industries allowing them to operate in continuous at the optimal operative conditions [27].

In this particular work, a single-cell DD module incorporating two anionic exchange membranes Fumasep FAD and Neosepta AFN were used to evaluate the recovery efficiency of sulphuric acid from both pure  $H_2SO_4$  and  $H_2SO_4/CuSO_4$  mixed solutions, mimicking the operating range of concentrations of a real case study at Electroniquel Co. (Spain). Batch tests with a recycle configuration were used to evaluate volume and concentration variations in both retentate and diffusate compartments and to characterize acid,  $Cu^{2+}$  and water transport through the AEM. Moreover, a mathematical model was constructed and validated to simulate the process and provide a design tool for the development of a pilot plant to be installed and tested in the real industrial site.

## **2. $H_2SO_4$ and $CuSO_4$ membrane transport in DD: mathematical model**

The mathematical model developed in this work was adapted from a model [28] for the recovery of HCl from HCl and  $FeCl_2$  solutions. The model incorporates: i) the steady-state spatial differential mass balance equations for a one-dimensional (1D) spatial discretization of the DD module along the two channels and; ii) the time differential equations considering the variation of concentration and volume in the two solutions (retentate and diffusate) tanks during batch operations. Figure 1 shows the diagram of a module that operates in countercurrent direction of length  $z_{ch}$  and surface membrane area  $A_m$ , where compartment I represents the retentate channel, while compartment II the diffusate one.  $C_{i,r}$  and  $C_{i,d}$  are the bulk concentrations of the i-component in the retentate and diffusate sides respectively;  $F_r$  and  $F_d$  are the volumetric flowrates in the retentate and diffusate channels respectively;  $J_i$  is the flux of the i-component through the membrane. The net water transport through an IEM derives from the contribution of osmosis and drag phenomena. The osmotic flux ( $J_{os}$ ) is due

to the osmotic pressure difference of between the two solutions, while the water drag ( $J_{dr}$ ) is due to the water transported in the solvation shell of the diffusing acid across the membrane.

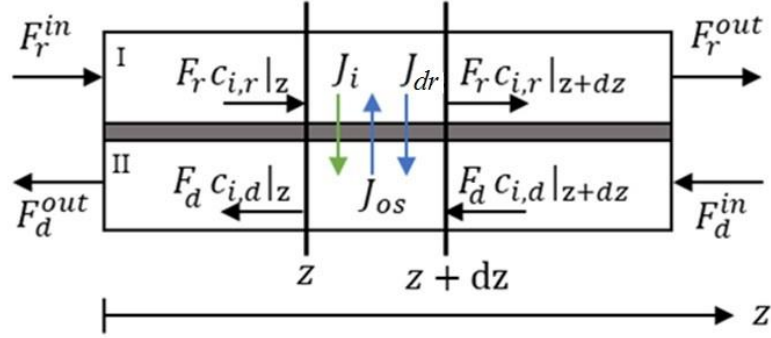


**Figure 1.** Schematic diagram of the discretized domain of the DD module in countercurrent configuration. Compartment I represents the retentate channel while compartment II the diffusate one [28].

Considering diffusive and convective mass transport under steady-state conditions, the variation of concentration along  $z$  in the two channels can be derived from the mass balance on the differential volume between  $z$  and  $z+dz$  (for the sake of brevity, only key equations for the retentate are reported, while further details could be found in ref [28]):

$$F_r c_{i,r}|_z = F_r c_{i,r}|_{z+dz} + J_i dA_m \quad (1)$$

$$dA_m = w_{ch} \cdot dz \quad (2)$$

$$\frac{dF_r c_{i,r}}{dz} = -J_i w_{ch} \quad (3)$$

$$\frac{dF_r}{dz} = \sum_i \frac{dF_r c_{i,r}}{dz} \frac{M_i}{\rho_r} \quad (4)$$

where  $w_{ch}$  is the channel width;  $\rho_r$  and  $M_i$  are density and molecular weight and of the retentate solution, respectively. The density was evaluated according to the model developed by Lalibertè et al. [29].

The boundary conditions for the two channels are:

$$z = 0 \quad c_{i,r} = c_{i,r}^{in} \quad (5)$$

$$z = z_{ch} \quad c_{i,d} = c_{i,d}^{in} \quad (6)$$

Mass transfer of i-component takes place through three resistances in series: i) through the boundary layer on the retentate side; ii) through the membrane; iii) through the boundary layer on the diffusate side. The total mass flux can be generally expressed as:

$$J_i = U_i \cdot \Delta C_i = U_i \cdot (C_{i,r} - C_{i,d}) \quad (7)$$

where  $U_i$  is the overall mass transfer coefficient of the i-component, defined as the reciprocal of the total resistance to the mass transfer:

$$U_i = \left[ \frac{1}{k_{i,r}} + \frac{1}{P_i} + \frac{1}{k_{i,d}} \right]^{-1} \quad (8)$$

where  $k_{i,r}$  and  $k_{i,d}$  are the mass transport coefficient for the i-component in retentate and diffusate channels and  $P_i$  is the permeability of the membrane for the i-component.

The presence of strong electrolytes (e.g.  $\text{CuSO}_4$ ) in the retentate solution can affect the flux of the acid. Thus, in the particular present case, the flux of  $\text{H}_2\text{SO}_4$  in the presence of  $\text{CuSO}_4$  can be expressed as:

$$J_{\text{H}_2\text{SO}_4}^{\text{tot}} = U_{\text{H}_2\text{SO}_4} \cdot (C_{\text{H}_2\text{SO}_4,r} - C_{\text{H}_2\text{SO}_4,d}) + U_{\text{CuSO}_4} \cdot (C_{\text{CuSO}_4,r} - C_{\text{CuSO}_4,d}) \quad (9)$$

where  $U_{\text{H}_2\text{SO}_4}$  is the overall mass transfer coefficient of the sulphuric acid,  $U_{\text{CuSO}_4}$  is the secondary overall mass transfer coefficient associated to the presence of copper salts and  $C_{\text{Cu}^{2+},r}$  and  $C_{\text{Cu}^{2+},d}$  are the salt concentrations in retentate and diffusate solutions, respectively. The salt flux can be expressed via the general transport equation:

$$J_{\text{Cu}^{2+}} = U_{\text{Cu}^{2+}} \cdot (C_{\text{Cu}^{2+},r} - C_{\text{Cu}^{2+},d}) \quad (10)$$

Where  $U_{\text{CuSO}_4}$  is the overall mass transfer coefficient of the copper sulphate.

The total water flux can be expressed as a contribution of osmotic and drag fluxes:

$$J_w = J_{os} + J_{dr} \quad (11)$$



The osmotic flux  $J_{os}$  can be calculated as:

$$J_{os} = P_w \cdot (\pi_r - \pi_d) \quad (12)$$

where  $P_w$  is the osmotic permeability of the membrane for water and  $\pi_r$  and  $\pi_d$  are the osmotic pressure in the retentate and diffusate side, respectively. Osmotic pressure was calculated with Pitzer model, instead of the Van't Hoff equation as used in [28]. According to Pitzer model [30], the osmotic pressure can be calculated as:

$$\pi = \frac{RTM_s\phi}{1000v_s} \cdot \sum im_i \quad (13)$$

where  $R$  is the gas universal constant,  $M_s$  is the solvent molecular weight,  $v_s$  is the molar volume of the solvent,  $i$  is the Van't Hoff coefficient,  $m_i$  is the molality of the  $i$ -component and  $\pi$  is the osmotic pressure. Osmotic coefficients ( $\phi$ ) and sulphuric acid and copper sulphate dissociation were evaluated by Pitzer equations [31-33].

At the tests operating in particular pH ( $\text{pH} < 1$ ) and for single sulphuric acid solutions ( $\text{H}_2\text{SO}_4$  concentration from 0.2 M to 2 M), the acid is present as a mixture of  $\text{HSO}_4^-$  (80 %) and  $\text{SO}_4^{2-}$  (20 %) (Figure 2a), while for sulphuric acid and copper sulphate solutions ( $\text{H}_2\text{SO}_4$  concentration from 0.6 M), the salt is present as a mixture of  $\text{Cu}^{2+}$  (60 %) and  $\text{CuSO}_{4\text{aq}}$  (40 %) (Figure 2b). According to this, the Van't Hoff coefficient for  $\text{H}_2\text{SO}_4$  was 2.2 and for  $\text{CuSO}_4$  was 1.5.

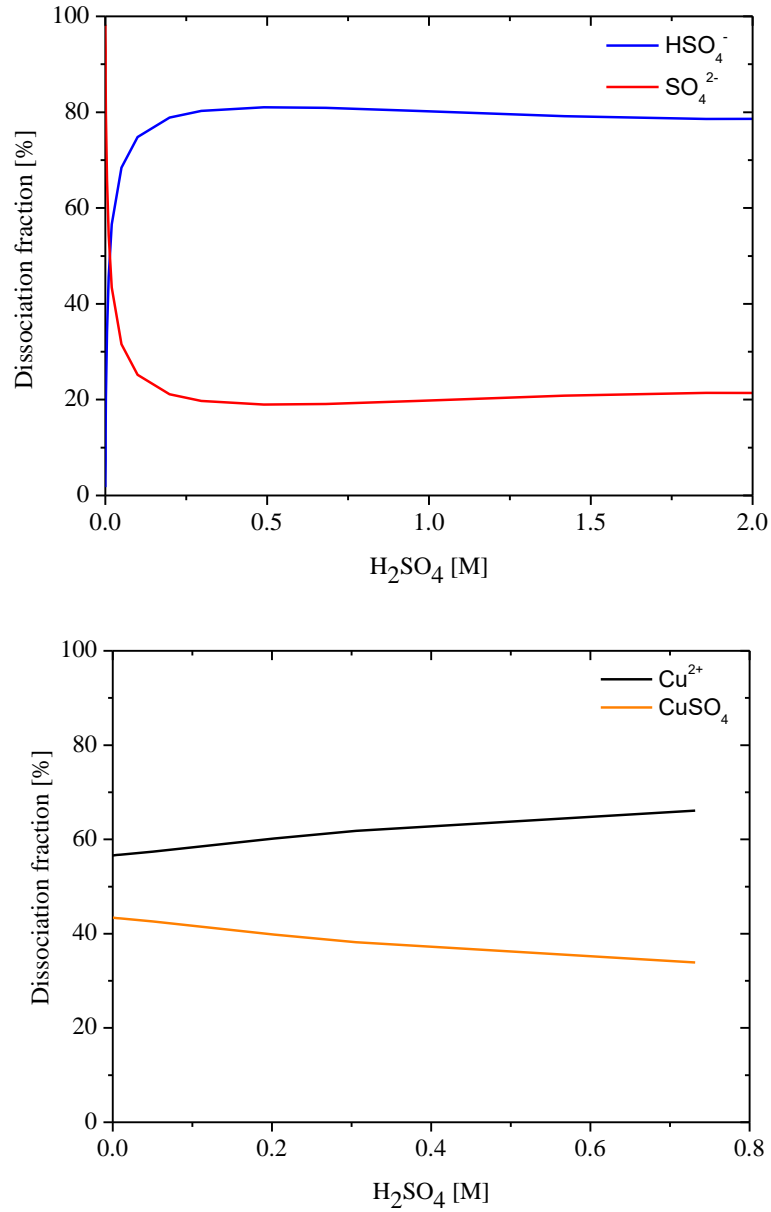


**Figure 2.** Calculated dissociation (%) of H<sub>2</sub>SO<sub>4</sub> (a) and CuSO<sub>4</sub> (b) as a function of acid concentration using Pitzer model.

The water drag flux is calculated as:

$$J_{dr} = \sum_i \beta_i \cdot J_i \quad (14)$$

where  $\beta_i$  is the solvation number of the species  $i$ . Solvation numbers adopted were 1 for H<sup>+</sup>, 8 for SO<sub>4</sub><sup>2-</sup> and 6 for Cu<sup>2+</sup> [34-37].

### 3. Experimental

### 3.1 Materials and methods

The feed retentate solutions were prepared from 96 wt% H<sub>2</sub>SO<sub>4</sub> solution (Honeywell), CuSO<sub>4</sub>·5H<sub>2</sub>O (Honeywell, purity ≥ 99%) and deionized water generated by a two-stage reverse osmosis unit (conductivity below 5 μS/cm). The feed diffusate solution was deionized water. H<sub>2</sub>SO<sub>4</sub> concentration was determined by titration with 0.01 and 0.1 M Na<sub>2</sub>CO<sub>3</sub> solutions (Carlo Erba reagents, purity ≥ 99.5%). The concentration of Cu<sup>2+</sup> was determined by iodometric titration, using KI (1 g), Na<sub>2</sub>S<sub>2</sub>O<sub>3</sub>·5H<sub>2</sub>O (0.1 M for retentate samples titrations and 0.0001 M for diffusate samples titrations) (Sigma-Aldrich, purity ≥ 99.5%) and starch as indicator (Carlo Erba reagents).

The DD unit was equipped first with a Fumasep type FAD AEM (Fumatech GmbH), whose main characteristics were reported in [28] and then with a Neosepta AFN (Table 1). The two feed channels were formed by a net polymeric spacer (Deukum GmbH), with open area 10 dm<sup>2</sup> and thickness 270 μm.

**Table 1.** Neosepta AFN membrane properties [38].

Characteristics	Unit	Value
Thickness	μm	160
Electric resistance	Ω cm <sup>2</sup>	0.5
Burst strenght	MPa	≥ 0.25
Temperature	°C	≤ 40
Stability	pH	0-8

### 3.2 Experimental set-up and procedure

Experiments were carried out in a purposely-developed laboratory set-up to evaluate the transport of sulphuric acid, copper sulphate and water through the AEM membrane in a batch operating mode with a recycle configuration (Figure 3).

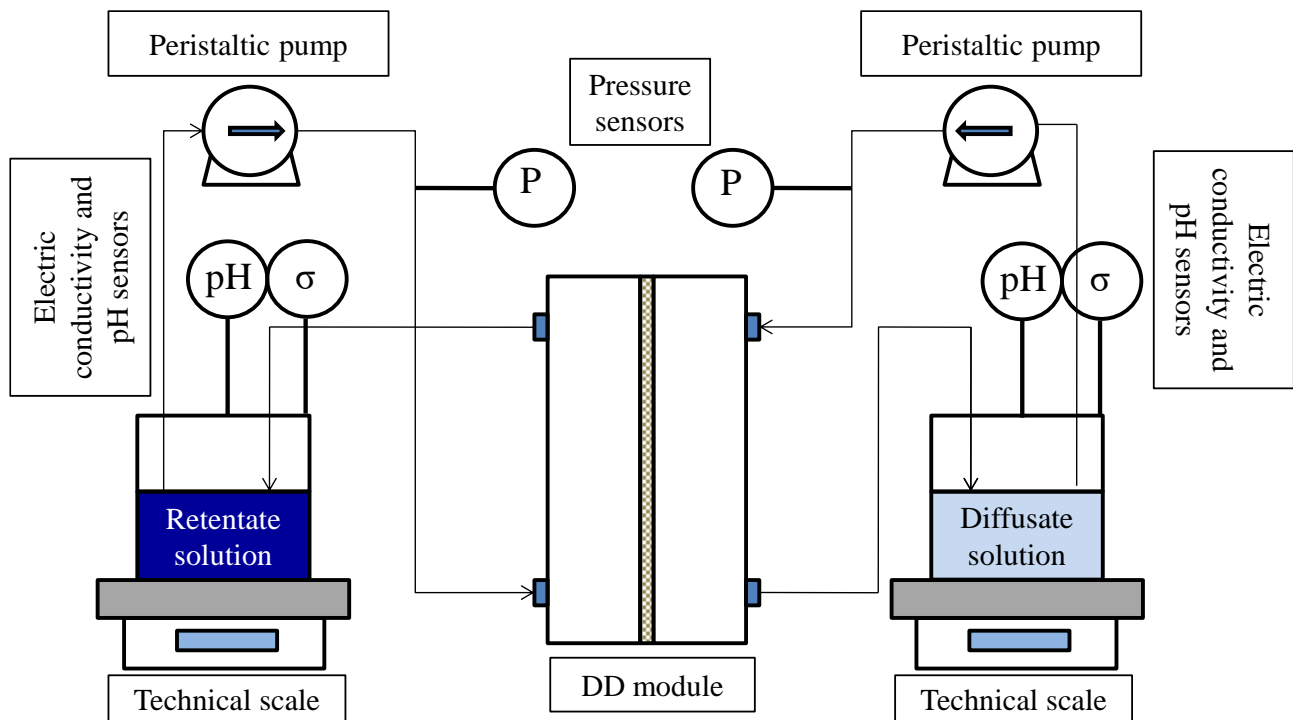


**Figure 3.** Experimental set-up for batch DD test equipment working in counter-current mode.

The set up was composed of a plate and frame DD module, two electronic scales (KERN, max 1000 g, 0.1 g sensibility) to measure the time variation of solutions mass during the experiment and two peristaltic pumps (Kronos KRFM-10). The DD module is made of two transparent polymethyl methacrylate (Plexiglas) plates of 20x20 cm<sup>2</sup> area and 5 cm thick. Distribution and collection of the fluid inside the module was attained by 6 screw holes of 12 <sup>1/4</sup>”, 3 inlets and 3 outlets.

Before any DD experiment, a solution with a concentration equal to the half of the retentate concentration was circulated through the two compartments of the module (retentate and diffusate) to condition the membrane for 120 min. Before starting the experiment, both compartments were rinsed with the retentate and diffusate solutions, respectively. At the beginning of each experiment, the retentate tank and the diffusate tank were filled with retentate solution and deionized water, respectively. The initial volume of solution in both tanks was 500 mL. All the experiments were performed with a constant flow rate (48 mL/min).

During each experiment, the concentration of acid and salt and the variation of total mass in both tanks were measured. In addition, pH and conductivity were measured by digital multi parameter

pH/conductivity-meter (Hanna Instruments) to monitor the experiments, checking that everything was working well. The acid and copper concentrations were measured after 1 h, then at intervals of 2 hours.

To monitor the pressure drops inside the module, a pressure gauge was connected to both inlet feed circuits. Water flux was determined by weight variation in the tanks. All the experiments were run at room temperature ( $22 \pm 2$  °C) and lasted 7 hours. To have a statistical relevance and calculate also the associated experimental error, each experiment was repeated from two to four times.

Operating and performance parameters as the acid flux ( $J_{H_2SO_4}$ ), copper flux ( $J_{Cu^{2+}}$ ),  $H_2SO_4$  recovery efficiency ( $\eta_{H_2SO_4}$ ) and copper rejection ( $Cu^{2+}$  Rejection) were calculated from experimental measurements by using Eqs. 15-19.

$J_{H_2SO_4}$  and  $J_{Cu^{2+}}$ , both of them variables along time, were calculated with the following equations:

$$J_{H_2SO_4} = \frac{d(V_d \cdot C_{H_2SO_4,d})}{A_m \cdot dt} \quad (15)$$

$$J_{Cu^{2+}} = \frac{d(V_d \cdot C_{Cu^{2+},d})}{A_m \cdot dt} \quad (16)$$

where  $V_d$  is the diffusate volume,  $C_{H_2SO_4,d}$  and  $C_{Cu^{2+},d}$  are the concentration of sulphuric acid and copper in diffusate side respectively and  $A_m$  is the surface membrane area.

$H_2SO_4$  Recovery is the actual acid recovery calculated as follow:

$$H_2SO_4 \text{ Recovery } (\%) = \frac{V_d \cdot C_{H_2SO_4,d}}{V_{r,0} \cdot C_{H_2SO_4,r,0}} \cdot 100 \quad (17)$$

where  $V_{r,0}$  is the initial volume of the retentate and  $C_{H_2SO_4,r,0}$  is the initial sulphuric acid concentration also in the retentate.

$H_2SO_4$  recovery efficiency was calculated with the following expression:

$$\eta_{H_2SO_4} (\%) = \frac{H_2SO_4 \text{ Recovery}}{H_2SO_4 \text{ Recovery,max}} \cdot 100 \quad (18)$$

where  $H_2SO_4 Recovery, max$  is the theoretical maximum acid recovery when the two solutions reach the equilibrium (in this particular case of equal feed tank volumes, this value is 50%).

And finally, the rejection of copper ( $Cu^{2+} Rejection$ ) was evaluated as:

$$Cu^{2+} Rejection (\%) = 100 - \frac{V_d \cdot C_{Cu^{2+},d}}{V_{r,0} \cdot Cr_{Cu^{2+},r,0}} \cdot 100 \quad (19)$$

where  $Cr_{Cu^{2+},r,0}$  is the initial copper concentration in the retentate.

### 3.3 Experimental plan

Three series of experimental runs were carried out with the Fumasep FAD membrane (Table 2). In several cases, results were compared with performances of a Neosepta AFN membrane. In the first one (from run 1 to run 6), the retentate solution was composed only by  $H_2SO_4$  at concentration from 0.2 to 2 M. In the second one (from run 7 to run 9), a solution of  $CuSO_4$  was used as retentate (concentration from 0.8 to 1.1 M), whereas, from run 10 to 13, performances of mixtures of  $H_2SO_4$  (0.6 M) and  $CuSO_4$  (from 0.2 to 1.1 M) solutions were studied. A  $H_2SO_4$  concentration of 0.6 M was selected to reproduce the reference operative conditions at Electroniquel copper electroplating plant (private communication, Electroniquel S. A.). For all the experiments, the circulating flow rate was 48 mL/min and deionized water was used as diffusate stream.

**Table 2.** Composition of feed retentate solution in the experimental runs.

Run	Retentate solution	
	[ $H_2SO_4$ ] [M]	[ $Cu^{2+}$ ] [M]
1*	0.2	0
2	0.4	0
3*	0.6	0
4	0.8	0
5*	1	0
6	2	0
7	0	0.8
8	0	0.9
9	0	1.1

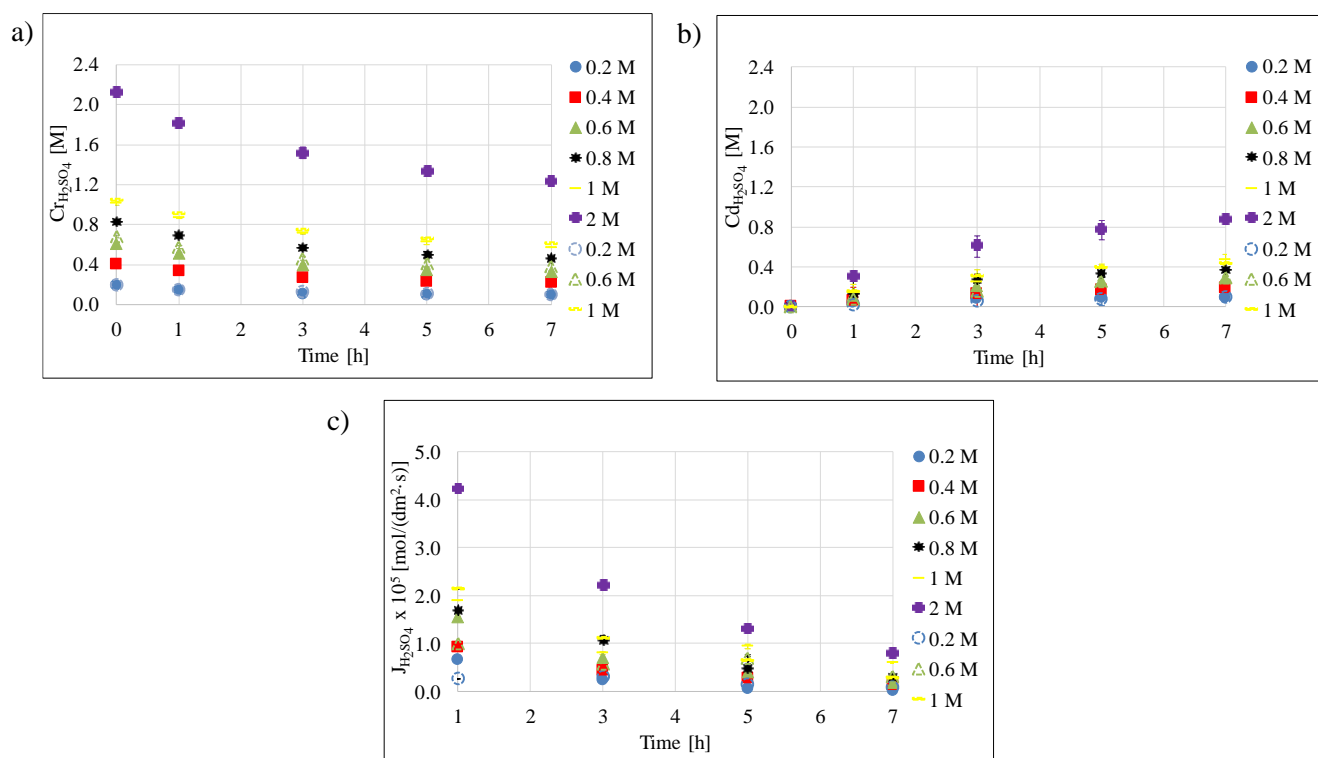
10*	0.6	0.2
11*	0.6	0.5
12	0.6	0.8
13*	0.6	1.1

\*Experiments carried out with both Fumasep FAD and Neosepta AFN.

## 4. Results and discussion

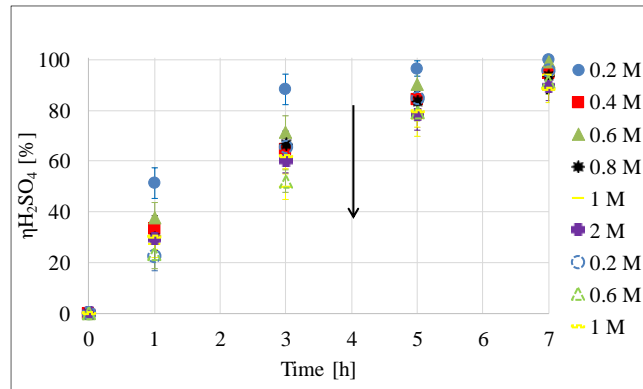
### 4.1 Diffusion Dialysis experiments with H<sub>2</sub>SO<sub>4</sub> solutions

The dependence of H<sub>2</sub>SO<sub>4</sub> concentration upon time is depicted in Figure 4a for the retentate and Figure 4b for the diffusate tank respectively, while the dependence of H<sub>2</sub>SO<sub>4</sub> flux ( $J_{H_2SO_4}$ ) upon time for the different H<sub>2</sub>SO<sub>4</sub> concentrations is shown in Figure 4c. The same trend can be observed for both membranes. The concentration of H<sub>2</sub>SO<sub>4</sub> in the retentate stream decreases during the experiment, while it increases in the diffusate as fast as higher is the initial acid concentration. When acid concentrations in the retentate and diffusate streams are equal, the acid passage stops, which occurs normally after 7 hours of operation. The acid flux increases with higher concentrations of H<sub>2</sub>SO<sub>4</sub> and it decreases upon time (Figure 4c), due to the reduction of the driving force.



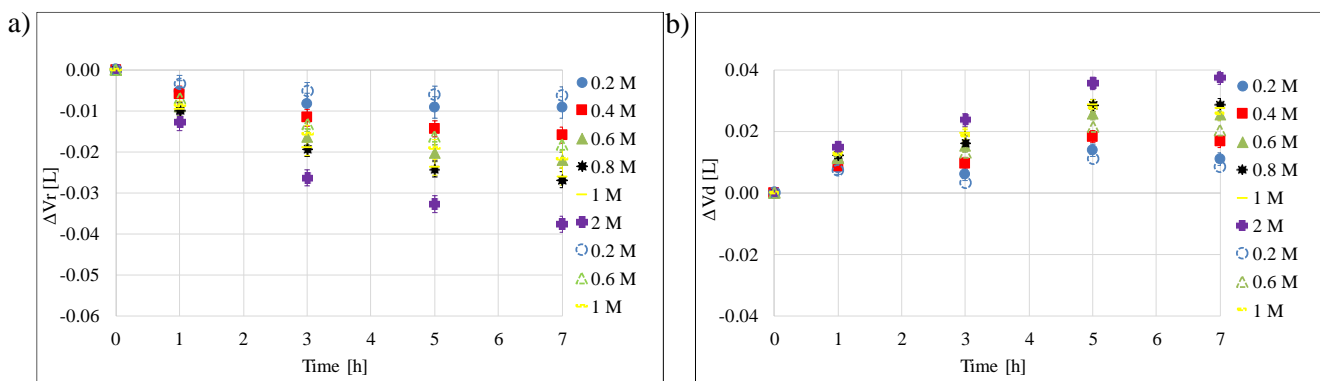
**Figure 4.** Variation of concentration in retentate solution ( $C_{r_{H_2SO_4}}$ ) (a), in diffusate solution ( $C_{d_{H_2SO_4}}$ ) (b) and of  $H_2SO_4$  flux ( $J_{H_2SO_4}$ ) (c) with time for different initial  $H_2SO_4$  concentrations: 0.2, 0.4, 0.6, 0.8, 1 and 2 M. Flow rate: 48 mL/min. Filled markers: Fumasep FAD and empty markers: Neosepta AFN.

Figure 5 shows the  $H_2SO_4$  recovery efficiency upon time for different initial acid concentrations in the retentate solution. The maximum efficiency is reached at the lowest concentration (0.2 M) and it increases with time. Several DD studies with strong acids have reported similar results [7, 24, 39]. The recoveries reached with Fumasep FAD are higher compared to those obtained with Neosepta AFN. The latter needed more time to reach the equilibrium.



**Figure 5.**  $H_2SO_4$  recovery efficiency ( $\eta_{H_2SO_4}$ ) as a function of time for different initial  $H_2SO_4$  concentrations: 0.2, 0.4, 0.6, 0.8, 1 and 2 M. Flow rate: 48 mL/min. Filled markers: Fumasep FAD and empty markers: Neosepta AFN. The arrow in the figure indicates the trend of  $\eta_{H_2SO_4}$  with the variation of  $H_2SO_4$  concentration.

Figure 6 represents the variation of volume over time in the retentate (Figure 6a) and diffusate (Figure 6b) solutions.





**Figure 6.** Variation of volume as a function of time in the retentate ( $\Delta V_r$ ) (a) and in the diffusate ( $\Delta V_d$ ) (b) for different initial  $H_2SO_4$  concentrations: 0.2, 0.4, 0.6, 0.8, 1 and 2 M. Flow rate: 48 mL/min. Filled markers: Fumasep FAD and empty markers: Neosepta AFN.

The same trend can be observed for both membranes. The volume of the retentate solution decreases while the volume of the diffusate increases for all acid concentrations studied. Therefore, the drag water flux from the retentate solution to the diffusate solution dominates against the osmotic flux and this is more evident as the initial acid concentration increases. In general, the retentate volume is higher and the diffusate volume is lower for Neosepta AFN respect to those for Fumasep FAD, evidencing a higher drag flux for the latter. The application of DD on acid recovery schemes is associated also to the objective of reaching the highest concentration values of acid on the diffusate. Accordingly, as the water transport associated to hydration has a higher contribution than the water transport due to the osmotic pressure, its value will be the ultimate factor to be considered when designing full scale DD operation. Developing of new membranes with properties limiting or reducing the transport associated to the ion hydration should be an objective.

#### 4.2 Influence of $CuSO_4$ on the $H_2SO_4$ transport

The AEM membrane performance to separate  $H_2SO_4$  from  $CuSO_4$  was also analyzed. At first, a preliminary set of experiments has been carried out with Fumasep FAD using only copper sulphate solution as retentate.  $Cu^{2+}$  rejection factor is reported as a function of time for the three different initial copper retentate concentrations (0.8, 0.9 and 1.1 M) in Figure 7.

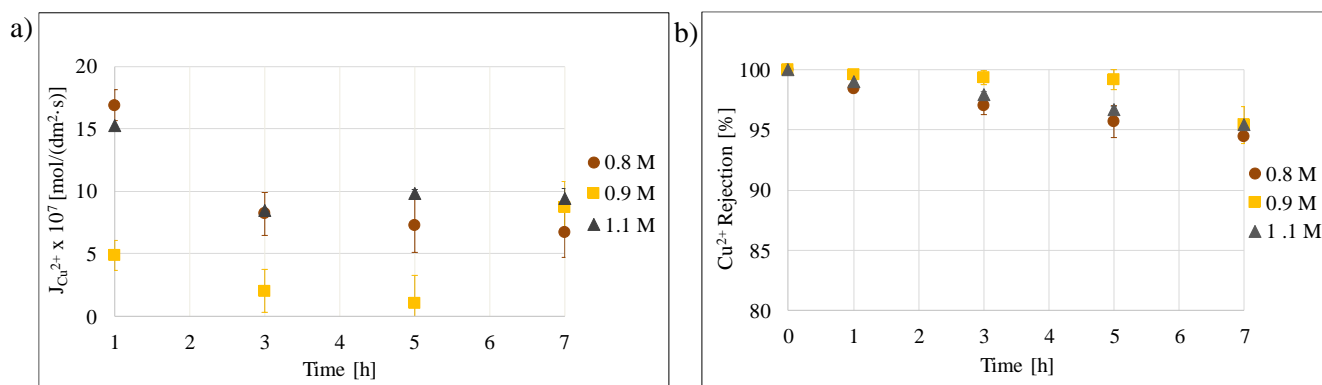


**Figure 7.** Copper flux ( $J_{Cu^{2+}}$ ) (a) and copper rejection ( $Cu^{2+}$  rejection) (b) as a function of time for different initial concentrations of copper: 0.8, 0.9 and 1.1 M. Flow rate: 48 mL/min<sup>-1</sup>. Retentate:  $CuSO_4 \cdot 5H_2O$  solution. Membrane: Fumasep FAD.

The copper flux was between  $10^{-6}$  and  $10^{-7}$  mol/(dm<sup>2</sup>·s) during all the experiment, more than one order of magnitude lower than that of the acid flux. Rejection values  $\geq 95\%$  were measured for all the concentrations after 7 hours. CuSO<sub>4</sub> is present in solution as Cu<sup>2+</sup> and non-charged form (CuSO<sub>4</sub>)<sub>aq</sub>, in a percentage of approximately 60 % and 40 % respectively (see section 2). Although the non-dissociated molecule has a larger size than the cation, it permeates through the membrane more easily because, in comparison to Cu<sup>2+</sup> that is repulsed by the positive charges of the AEM quaternary ammonium functional groups, the non-charged form is not affected by any electrical repulsion. The absence of Cu<sup>2+</sup> negative complexes, the higher concentration of preferred co-transported cation (H<sup>+</sup>) and the large size of the non-dissociated species (CuSO<sub>4aq</sub>) favour the Cu<sup>2+</sup> rejection by the membrane [17].

To study the effect of CuSO<sub>4</sub> on the H<sub>2</sub>SO<sub>4</sub> recovery, a set of experiments with a constant acid concentration of 0.6 M and different concentrations of Cu<sup>2+</sup> (0.2, 0.5, 0.8 and 1.1 M) was carried out. Figure 8 shows H<sub>2</sub>SO<sub>4</sub> recovery efficiency ( $\eta_{H_2SO_4}$ ) (a) and Cu<sup>2+</sup> rejection (b) upon time for a constant initial acid concentration of 0.6 M for different initial copper concentrations using both membranes.

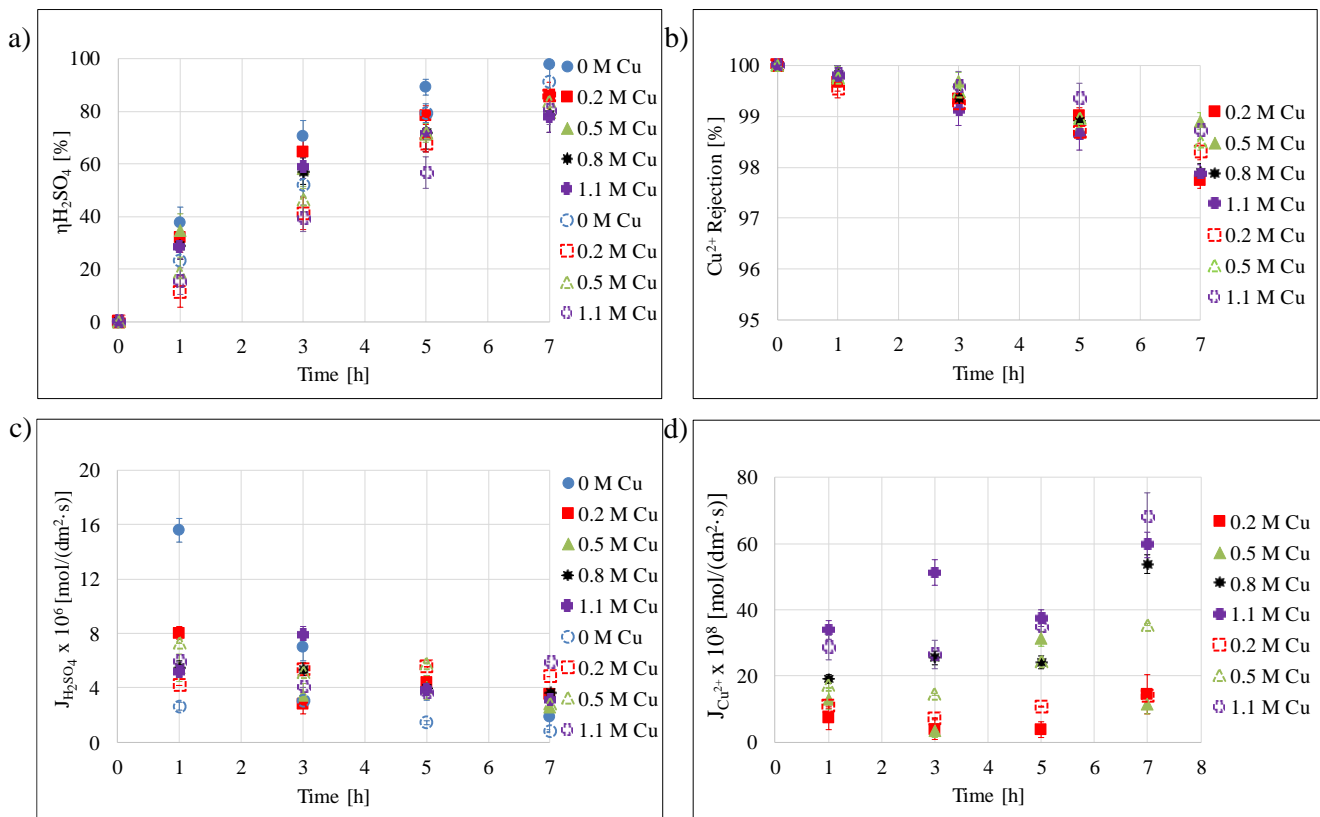


**Figure 8.** H<sub>2</sub>SO<sub>4</sub> recovery efficiency ( $\eta_{H_2SO_4}$ ) (a), Copper rejection (Cu<sup>2+</sup> rejection) (b), H<sub>2</sub>SO<sub>4</sub> flux ( $J_{H_2SO_4}$ ) (c) and copper flux ( $J_{Cu^{2+}}$ ) (d) as a function of time at a constant initial H<sub>2</sub>SO<sub>4</sub> concentration of 0.6 M, for different initial copper concentrations: 0, 0.2, 0.5, 0.8 and 1.1 M. Flow rate: 48 mL/min. Filled markers: Fumasep FAD and empty markers: Neosepta AFN.

As expected, Cu<sup>2+</sup>, which is mainly present as Cu<sup>2+</sup> and CuSO<sub>4(aq)</sub> is preferentially rejected compared with the fastest cation H<sup>+</sup> in the co-transportation with HSO<sub>4</sub><sup>-</sup>. Non-charged species as CuSO<sub>4</sub>, could not be co-transported with HSO<sub>4</sub><sup>-</sup> for charge compensation as it occurs for protonated forms of acids, [4] and, due to their large size, they could present more difficulties of diffusing in the membrane than smaller ones [39].

After 7 hours, Cu<sup>2+</sup> rejection (Figure 8 b) is maintained at 97 % for all Cu<sup>2+</sup> concentrations tested. It is higher compared to the result obtained in the experiments without acid (95 %), thus indicating that the presence of H<sub>2</sub>SO<sub>4</sub> decreases the copper transport through the membrane. This behaviour has been also reported by Palatý and Záková using Neosepta AFN membrane [22] and can be attributed to the anionic nature of the membrane that favours the passage of sulphate anions over that of copper cations (Figure 8 c and d) and assuming this large molecule an obstacle to the passage of the cation. For what concern the recovery of H<sub>2</sub>SO<sub>4</sub> (Figure 8 a), the presence of Cu<sup>2+</sup> has a slightly negative effect. For example, at the end of the experiment (7 h), the  $\eta_{H_2SO_4}$  for Fumasep FAD decreased a 10 % at 0.2 M Cu<sup>2+</sup> and this change was even larger for 1.1 M (20 %), whereas these changes were smaller for Neosepta AFN (5 % at 0.2 M Cu<sup>2+</sup>, and 12 % at 1.1 M Cu<sup>2+</sup>). Comparing with the results obtained at the end of the experiment without the presence of Cu<sup>2+</sup>, the  $\eta_{H_2SO_4}$  is reduced from 10 % to 20 % when concentration varies from 0.2 to 1.1 M respectively, when Fumasep FAD is used and between 5 % and 12 % with Neosepta AFN for the same range of Cu<sup>2+</sup> concentration. Moreover, after 7 hours, the recovery for both membranes is practically the same evidencing a greater effect of the presence of copper for Fumasep FAD. Although there is no formation of negative complexes that compete for the passage through the membrane, the presence of copper sulphate in the form of non-dissociate species can hinder the passage of anions due to the large size of CuSO<sub>4(aq)</sub>, as reported also by Bendová and Palatý using Neosepta AFN [25].

When the volume variations are considered, results are obtained concerning the net water flux from the retentate to the diffusate solution (see Figure 9).

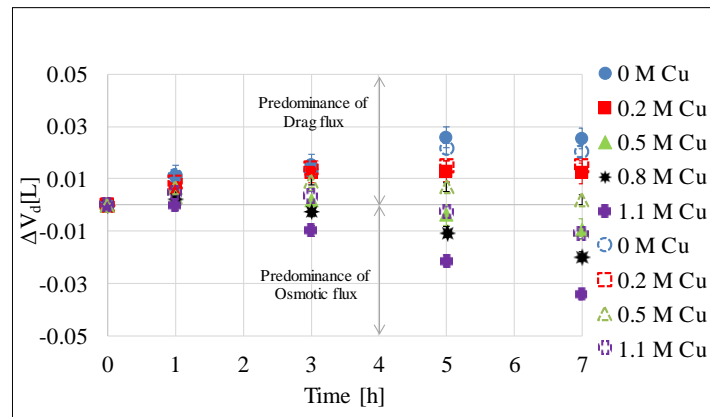


**Figure 9.** Variation of the volume as a function of time in the diffusate ( $\Delta V_d$ ) at a constant initial  $\text{H}_2\text{SO}_4$  concentration of 0.6 M for different initial copper concentrations: 0, 0.2, 0.5, 0.8 and 1.1 M. Flow rate: 48 mL/min. Filled markers: Fumasep FAD and empty markers: Neosepta AFN.

During the first hour, the diffusate volume increases due to the prevalence of the drag flux for all copper concentrations and for both membranes. However, after this hour, the osmotic behaviour is different depending on the copper concentration and the membrane. For Fumasep FAD, from the third hour, the osmotic flux starts to be significant, being more evident as the copper concentrations increase. This is a common behaviour for solutions with strong electrolytes, because the increase of ionic strength increases the osmotic pressure on the retentate side favouring the water flux from the diffusate to the retentate. For Neosepta AFN, the osmotic flux is lower and the effect of the presence of copper is less accused. The prevalence of osmotic flux is only observed after 5 hours for a concentration of 1.1 M and it starts to be significant after 7 hours for 0.5 M copper concentration.

#### 4.3. DD transport model for $\text{H}_2\text{SO}_4/\text{CuSO}_4$ mixtures through Fumasep FAD: calibration and validation

As it has been reported elsewhere [9, 20, 22, 28], in solutions of strong electrolytes (e.g.  $\text{H}_2\text{SO}_4$  bath) the permeability of membrane for acid and water is correlated to the retentate concentration of the acid. The model is calibrated by determining a correlation for the permeability of the membrane for

acid and for water related to the acid concentration in the retentate solution and for  $\text{Cu}^{2+}$  as a function of  $\text{Cu}^{2+}$  concentration also in the retentate solution (Figure 10 a and b). In all the experiments, linear correlations for the acid ( $P_{H_2SO_4}$ ) and for the water ( $P_w$ ) permeabilities provide a good fitting between experimental and model data. Then, all these linear correlations are used to obtain a unique correlation for the permeability of the membrane for acid (eq. 20) and for water (eq. 21) as a function of the acid concentration in the retentate solution (Figure 10 a and b):

$$P_{H_2SO_4} = 6.8 \cdot 10^{-6} \cdot Cr_{H_2SO_4}^{-1} + 2.2 \cdot 10^{-5} \quad (\text{deviation of } 5.4 \cdot 10^{-6}) \quad (20)$$

$$P_w = 1.9 \cdot 10^{-8} \cdot Cr_{H_2SO_4}^{-1} + 8.8 \cdot 10^{-8} \quad (21)$$

$P_{H_2SO_4}$  and  $P_w$  decrease as the acid concentration in the retentate solution increases. This fact explains the lower  $\text{H}_2\text{SO}_4$  recovery efficiency obtained by increasing the acid concentration (section 4.1). Also Palatý and Bendová [13] reported the same permeability trend using a Fumasep FAD membrane. This phenomenon can be ascribed to the size of the  $\text{H}_2\text{SO}_4$  generated anions ( $\text{HSO}_4^-$ ), that are higher than those for halogenated acids as  $\text{HF}$  ( $\text{F}^-$ ),  $\text{HCl}$  ( $\text{Cl}^-$ ) or  $\text{HBr}$  ( $\text{Br}^-$ ). In fact, the bigger is the anion to be transported through the AEM, the lower is its mobility in the membrane. In this case, an increase of the concentration has a negative influence, as also observed for the recovery of phosphoric acid using a Fumasep FAD AEM (the permeability decreased from  $3.26 \cdot 10^{-5}$  m/s to  $0.67 \cdot 10^{-5}$  m/s when the concentration varied from 0.2 M to 2 M) [40]. Moreover, an increase of the acid concentration causes an increase in ionic strength reducing the mobility of the transport ions in the membrane. This produces a decrease of the permeability [20]. Also, this may be due to the osmotic water transport and the dehydration of the membrane. A higher acid concentration causes a decrease in membrane swelling with the corresponding membrane dehydration resulting in the increasing frictional resistance to ion transport at high concentration [24, 39]. Moreover, the transport of  $\text{H}_2\text{SO}_4$  may be controlled by diprotic acid ionization [24, 39]. According to dissociation constant of  $\text{H}_2\text{SO}_4$ , the monovalent  $\text{HSO}_4^-$  is the dominant specie. The negative charge of  $\text{SO}_4^{2-}$  ion is higher than that of

leading to  $\text{HSO}_4^-$  ion had higher friction resistance for the same operating conditions [39]. Finally, the membrane may have a limit in the ion exchange capacity [24].

The permeability of the membrane for  $\text{Cu}^{2+}$  ( $P_{\text{Cu}^{2+}}$ ) (eq. 22) is calibrated following a similar procedure. However, differently from the acid and water, a constant value for each experiment was considered instead of a linear correlation. Then, all these constant values are used to obtain a unique correlation for the permeability of the membrane for copper as a function of the copper concentration in the retentate solution (Figure 10 c).

$$P_{\text{Cu}^{2+}} = 2.4 \cdot 10^{-7} \cdot Cr_{\text{Cu}^{2+}} + 1.8 \cdot 10^{-7} (\text{deviation of } 9 \cdot 10^{-8}) \quad (22)$$

With regard to the copper permeability, this increases as the  $\text{CuSO}_4$  concentration increases and, as expected, it is two orders of magnitude lower than  $P_{\text{H}_2\text{SO}_4}$

Finally, a secondary overall mass transfer coefficient ( $Us_{\text{H}_2\text{SO}_4}$ ) is evaluated to take into account the effect of  $\text{CuSO}_4$  on  $\text{H}_2\text{SO}_4$  flux. However, for all the concentrations,  $Us_{\text{H}_2\text{SO}_4}$  shows a value of four orders of magnitude lower than the  $P_{\text{H}_2\text{SO}_4}$ , thus the effect of this term on the acid flux can be neglected in the model (Figure 10 d).

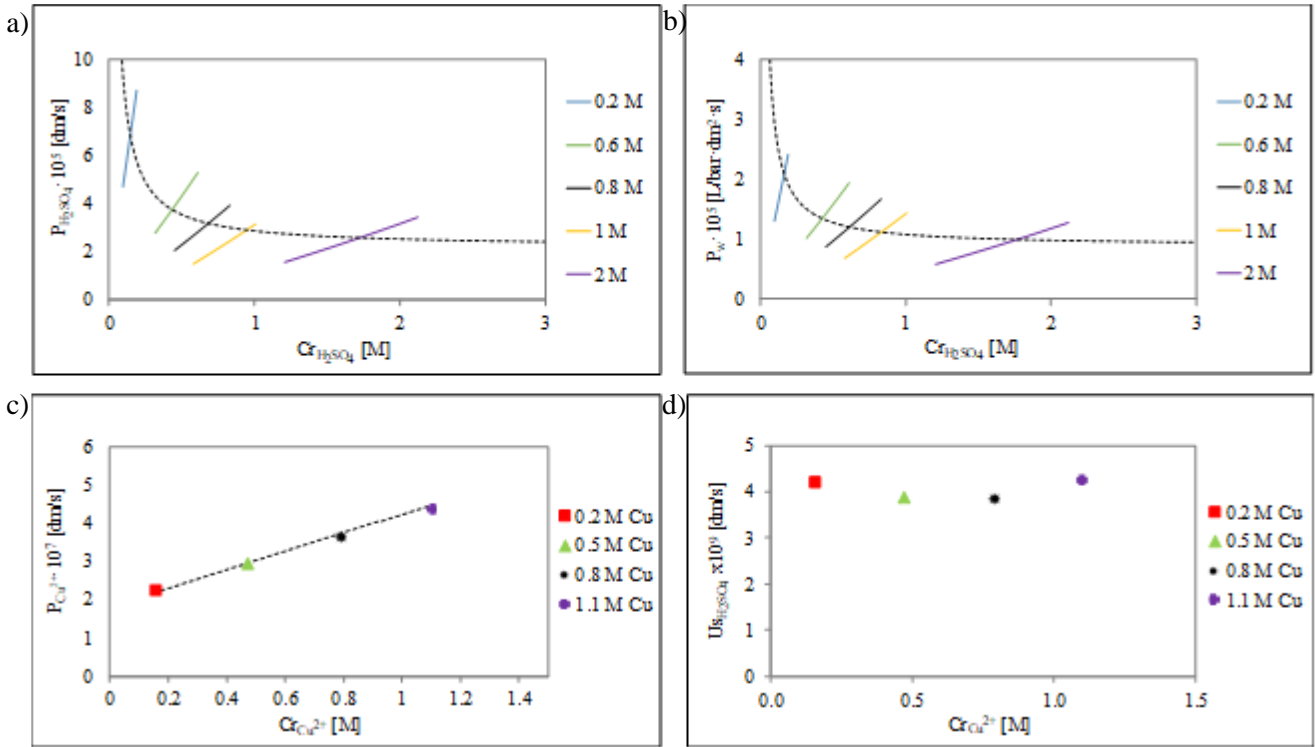


**Figure 10.** Linear correlations (continuous line) and unique correlation (dashed curve) of permeability of the membrane for H<sub>2</sub>SO<sub>4</sub> ( $P_{H_2SO_4}$ ) (a) and for water ( $P_w$ ) (b) upon the initial H<sub>2</sub>SO<sub>4</sub> concentration in the retentate and of permeability of the membrane for Cu<sup>2+</sup> ( $P_{Cu}$ ) (c) and secondary overall mass transfer coefficient ( $US_{H_2SO_4}$ ) (d) upon the initial Cu<sup>2+</sup> concentration in the retentate solution. Membrane: Fumasep FAD.

Concerning the water flux, in particular the osmotic flux, in addition to the correlation for the permeability of the membrane for the water, another correlation for the osmotic pressure in the retentate and diffusate solutions as a function of the acid and copper concentrations in the respective solutions is adjusted. To obtain the correlation (Eq.23), a value of osmotic pressure (Eq.13) is obtained for each value of acid concentration (range from 0.1 M to 0.8 M) and Cu<sup>2+</sup> concentration (range from 0 M to 1.15 M).

$$\pi_{r/d} = 0.5 + 36 \cdot Cr/d_{H_2SO_4} + 20.4 \cdot Cr/d_{CuSO_4} - 6.75 \cdot Cr/d_{H_2SO_4} \cdot Cr/d_{CuSO_4} \quad (23)$$

where  $Cr/d_{H_2SO_4}$  and  $Cr/d_{CuSO_4}$  are the H<sub>2</sub>SO<sub>4</sub> and CuSO<sub>4</sub> molar concentrations respectively in retentate/diffusate solutions.

For the drag flux, a hydration shell of 10 for  $\text{H}_2\text{SO}_4$  and 14 for  $\text{CuSO}_4$  are considered (Eq. 14). These hydration shell number for both electrolytes are derived taking into account the individual values of the corresponding ions (section 2).

Then, the model is validated by comparing the calculated acid and copper concentrations and volumes in the retentate and in the diffusate for all the DD experiments (see Table 2) against the experimental values obtained (Figure 11).

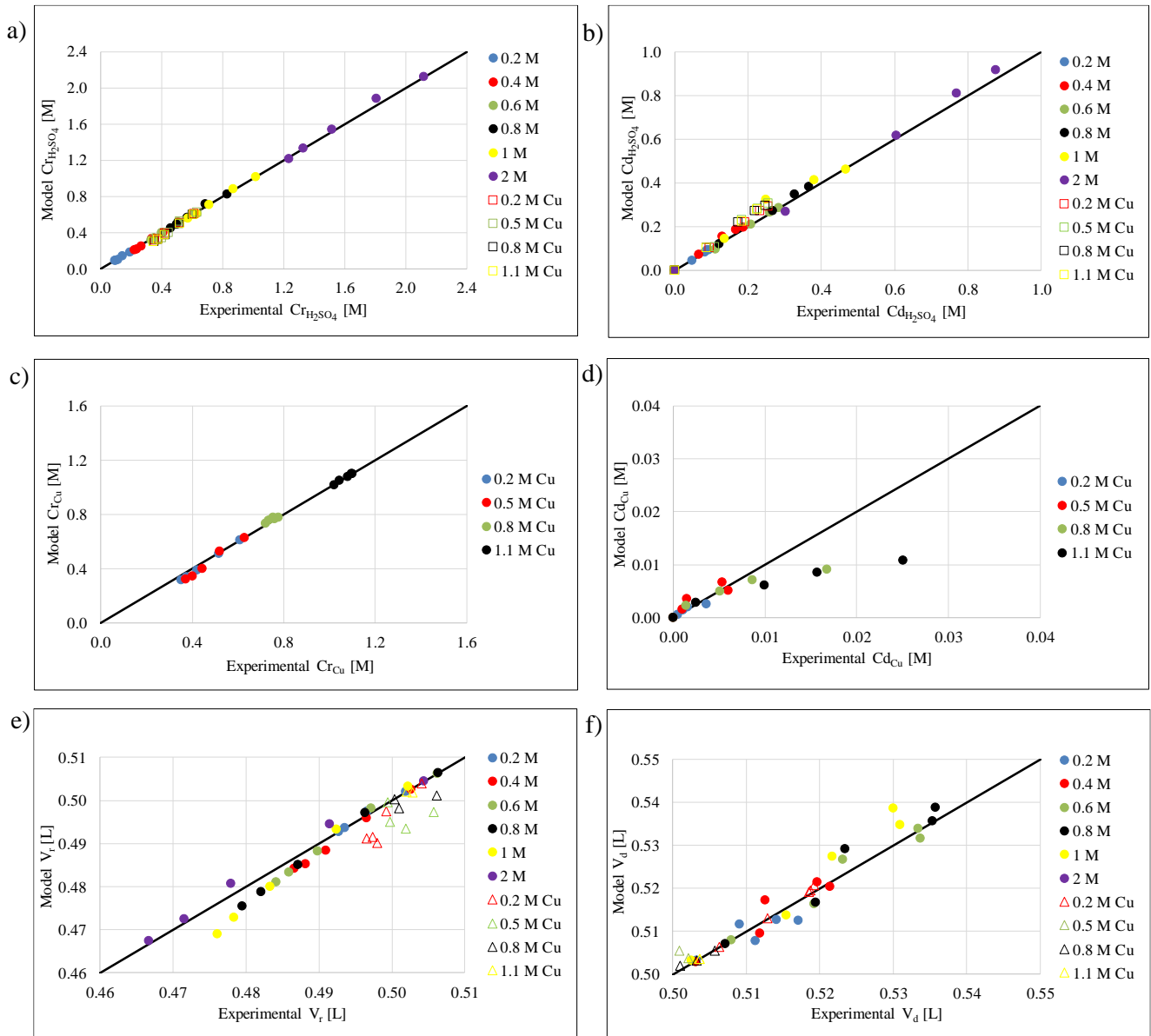


**Figure 11.** Comparison of calculated retentate (a) and diffusate (b)  $\text{H}_2\text{SO}_4$  concentrations, of calculated retentate (c) and diffusate (d) Cu concentrations and of retentate (e) and diffusate (f) volumes versus experimental data. (a) and (b) tests with single  $\text{H}_2\text{SO}_4$  at 0.2, 0.4, 0.6, 0.8, 1 and 2 M and with  $\text{Cu}^{2+}$  at a constant initial  $\text{H}_2\text{SO}_4$  concentration of 0.6 M. (c) and (d) tests with  $\text{Cu}^{2+}$  at 0.2,



0.5, 0.8 and 1.1 M at a constant initial  $H_2SO_4$  concentration of 0.6 M. (e) and (f) tests with single  $H_2SO_4$  at 0.2, 0.4, 0.6, 0.8, 1 and 2 M and with  $Cu^{2+}$  at 0.2, 0.5, 0.8, and 1.1 M at a constant initial  $H_2SO_4$  concentration of 0.6 M. Membrane: AEM Fumasep FAD.

As can be observed, a good agreement exists between measured and model estimates for the different solutions evaluated. It is of mention also that the predicted values of  $Cu^{2+}$  concentrations on the diffusate channel, especially for the more concentrated solutions, slightly deviate from the model. However, this deviation can be considered acceptable because the passage of  $Cu^{2+}$  through the membrane is very low (maximum experimental value 0.025 M).

#### 4.4. DD transport model for $H_2SO_4/CuSO_4$ mixtures through Neosepta AFN: calibration and validation.

The same procedure is used to evaluate AEM Neosepta AFN performances. Figure 12 show the calibration permeabilities of the membrane for the acid, for the water and for the  $Cu^{2+}$ . Again,  $U_{S_{H_2SO_4}}$  shows a value of four orders of magnitude lower than the  $P_{H_2SO_4}$ , thus the effect of this term on the acid flux could be neglected in the model.

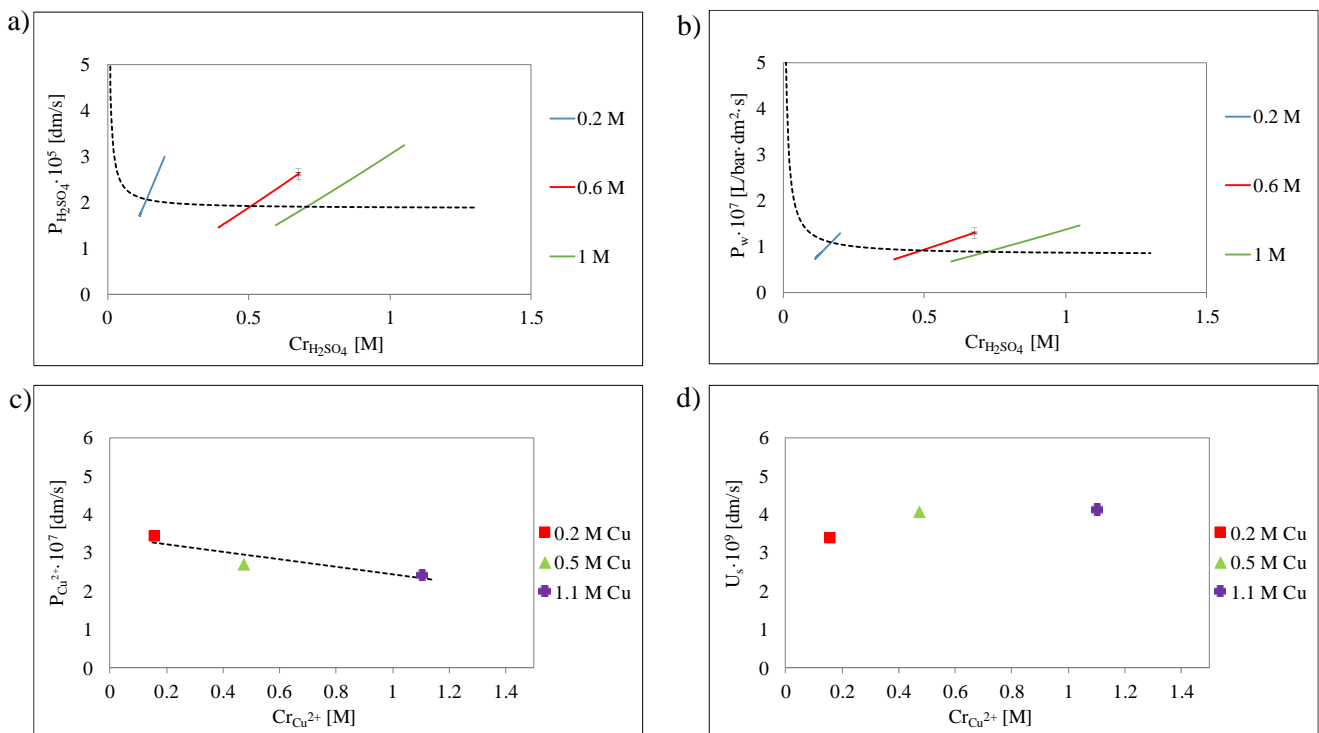


**Figure 12.** Linear correlations (continuous line) and unique correlation (dashed curve) of permeability of the membrane for H<sub>2</sub>SO<sub>4</sub> ( $P_{H_2SO_4}$ ) (a) and for water ( $P_w$ ) (b) upon the initial H<sub>2</sub>SO<sub>4</sub> concentration in the retentate and of permeability of the membrane for Cu<sup>2+</sup> ( $P_{Cu}$ ) (c) and secondary overall mass transfer coefficient ( $U_{S_{H_2SO_4}}$ ) (d) upon the initial Cu<sup>2+</sup> concentration in the retentate solution. Membrane: AEM Neosepta AFN.

The correlations for the permeability of the membrane for the acid, for the water and for the Cu<sup>2+</sup> are the following:

$$P_{H_2SO_4} = 2.7 \cdot 10^{-7} \cdot Cr_{H_2SO_4}^{-1} + 1.9 \cdot 10^{-5} \text{ (deviation of } 6.1 \cdot 10^{-6}) \quad (24)$$

$$P_w = 4.6 \cdot 10^{-9} \cdot Cr_{H_2SO_4}^{-1} + 8.2 \cdot 10^{-8} \quad (25)$$

$$P_{Cu^{2+}} = -9.8 \cdot 10^{-8} \cdot Cr_{Cu^{2+}} + 3.4 \cdot 10^{-7} \text{ (deviation of } 7.5 \cdot 10^{-8}) \quad (26)$$

The trend of  $P_{H_2SO_4}$  and  $P_w$  is the same than that for Fumasep FAD membrane, namely, a decrease of them as the acid concentration in the retentate solution increases. As in the case of Fumasep FAD membrane, the model is validated by comparing the calculated acid and copper concentrations and volumes in the retentate and in the diffusate for all the DD experiments (see Table 2) against the experimental values obtained (Figure 13). In all the cases, the use of the equations 24-26 results in a good agreement between model and experiments.

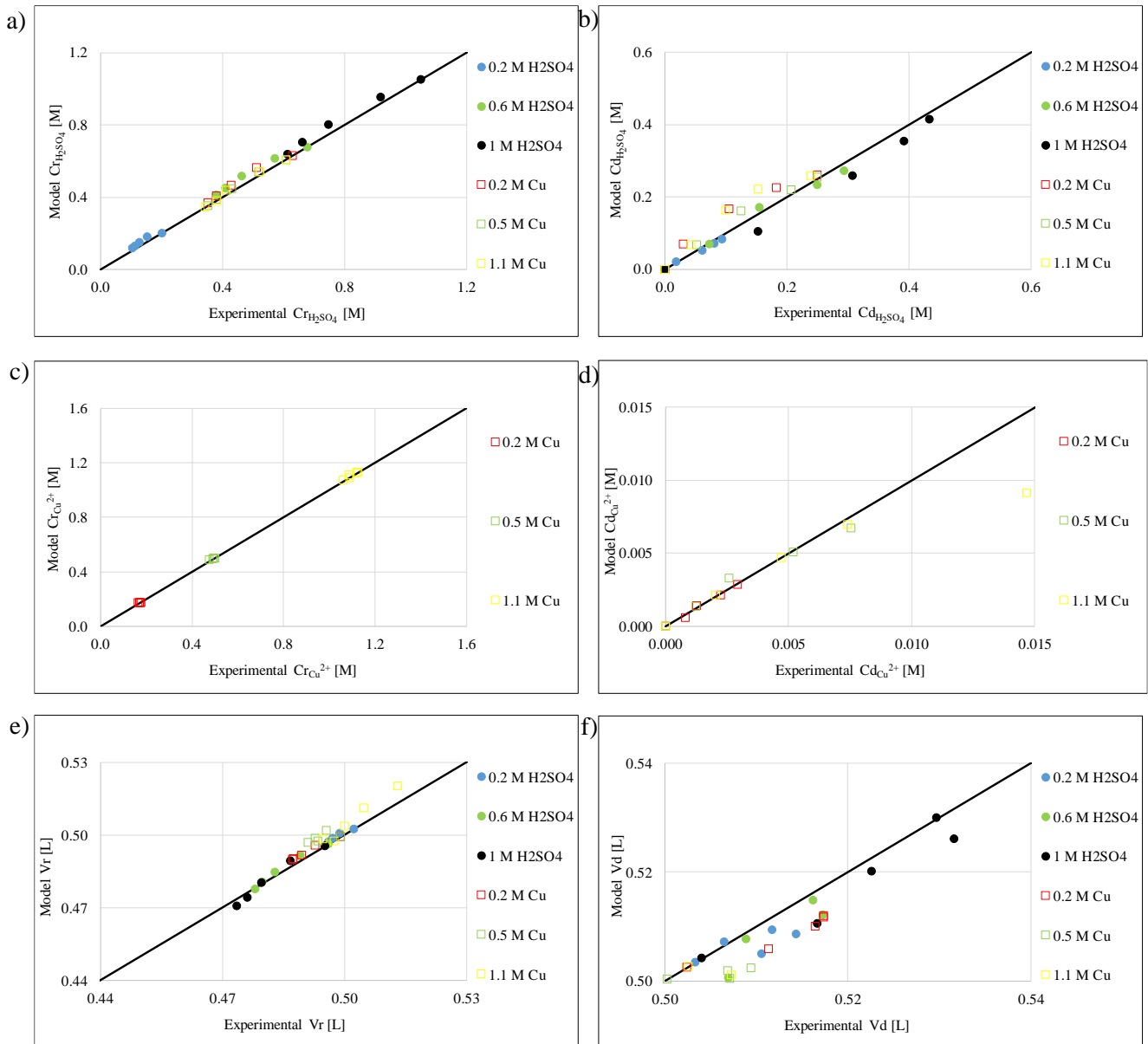


**Figure 13.** Comparison of calculated retentate (a) and diffusate (b)  $\text{H}_2\text{SO}_4$  concentrations, of calculated retentate (c) and diffusate (d) Cu concentrations and of retentate (e) and diffusate (f) volumes versus experimental data. (a) and (b) tests with single  $\text{H}_2\text{SO}_4$  at 0.2, 0.4, 0.6, 0.8, 1 and 2 M and with  $\text{Cu}^{2+}$  at a constant initial  $\text{H}_2\text{SO}_4$  concentration of 0.6 M. (c) and (d) tests with  $\text{Cu}^{2+}$  at 0.2, 0.5, 0.8 and 1.1 M at a constant initial  $\text{H}_2\text{SO}_4$  concentration of 0.6 M. (e) and (f) tests with single  $\text{H}_2\text{SO}_4$  at 0.2, 0.4, 0.6, 0.8, 1 and 2 M and with  $\text{Cu}^{2+}$  at 0.2, 0.5, 0.8, and 1.1 M at a constant initial  $\text{H}_2\text{SO}_4$  concentration of 0.6 M. Membrane: Neosepta AFN.

By comparing the results obtained for the two AEMs membranes (Fumasep FAD and Neosepta AFN), as shown in Table 4, concerning the acid permeability, AEM Fumasep FAD exhibits a higher value than that for the AEM Neosepta AFN. However, the trend for the  $\text{Cu}^{2+}$  permeability is different, while for Fumasep FAD, the value increases with a higher concentration, for Neosepta FAD, the effect of

the increasing concentration of  $\text{Cu}^{2+}$  affects the permeability negatively. The range of the values is closer than that for the permeability of the membranes for the acid. Comparing with the values obtained by other authors, the stirring of the retentate solution favours the permeability of the anions versus the batch recycle of the solution. This is due to the fact that stirring favours the convective mass transfer.

**Table 4.** Comparison of permeability of Fumasep FAD and Neosepta AFN obtained in this work with those obtained by other authors.

Membrane AEM	Concentration Range [M]	Operation Configuration	$P_{\text{H}_2\text{SO}_4} \cdot 10^{-5}$ [dm/s]	$P_{\text{Cu}^{2+}} \cdot 10^{-7}$ [dm/s]	Ref
Fumasep FAD	0.2-2 $\text{H}_2\text{SO}_4$ 0.2-1.1 $\text{Cu}^{2+}$	Bath recirculation	5.6-2.5	2.3-4.5	This work
Fumasep FAD	0.2-2 $\text{H}_2\text{SO}_4$	Two compartments batch stirred dialyzer	24.4-8.7	-	[13]
Neosepta AFN	0.2-1 $\text{H}_2\text{SO}_4$ 0.2-1.1 $\text{Cu}^{2+}$	Bath recirculation	2.1-1.9	3.2-2.3	This Work
Neosepta AFN	0.1 $\text{H}_2\text{SO}_4$	Two compartments batch stirred dialyzer	4.6	-	[14]
Neosepta AFN	0.1-1 $\text{H}_2\text{SO}_4$ 0.1-1 $\text{Cu}^{2+}$	Continuous dialyzer	3.1	22	[25]

## 5. Conclusions

In this study, the AEMs Fumasep FAD and Neosepta AFN are evaluated in the DD process to recover sulphuric acid and separate from copper sulphate, being for the Fumasep FAD the first time. A very high  $\text{H}_2\text{SO}_4$  recovery efficiency (89-100 %, ) is obtained with both membranes and it is higher when the acid concentration is lower. Moreover, a very high copper rejection equal to 95 % is obtained with Fumasep FAD. However, the presence of  $\text{CuSO}_4$  in the acid solution slightly negatively influences the acid recovery but the rejection of the metal increases up to 97 to 99 %. Therefore, Fumasep FAD and Neosepta AFN membranes are suitable for the separation of  $\text{H}_2\text{SO}_4$  and  $\text{CuSO}_4$  since it allows a

high recovery of acid and a high rejection of the copper salt. The permeability for the acid and for water are higher for Fumasep one leading to a higher value of  $\eta_{H_2SO_4}$ . For the case of the passage of  $Cu^{2+}$ , the permeability of the membrane is also slightly greater, so, the rejection of  $Cu^{2+}$  is also slightly lower than that for Neosepta AFN. The osmotic flux is also higher for Fumasep FAD membrane.

Finally, a mathematical model using time/space distributed-parameters is developed for both AEMs and they are calibrated and validated using the experimental results. In fact, a very good fitting between experimental data and model predictions is obtained for the two AEMs. The model results to be a useful tool able to be used for the development of the pilot plant that will be installed in Electroniquel S. A. company.

### **Acknowledgement**

This work was financially supported by EU within the ReWaCEM project (Resource recovery from industrial Wastewater by Cutting Edge Membrane technologies) – Horizon 2020 program, Grant Agreement no. 723729.

The authors are greeting to DEUKUM GmbH and Fumatech GmbH for supporting the DD stack assembly and providing the AEM membranes.

This mobility period of Julio López at the University of Palermo was supported by the Spanish Ministry (MINECO), within the scope of the grant BES-2015-075051, inside the Waste2Product project (CTM2014-57302-R), financed by the Ministerio de Economía y Competitividad (MINECO) and the Catalan Government (Project Ref. 2014SGR50) of Spain.

### **Acronyms**

AEM	Anion Exchange Membrane
BPPO	Brominated poly (2,6-dimethyl 1,4-phenylene oxide)
CEM	Cation Exchange Membrane
DD	Diffusion Dialysis
IEM	Ion Exchange Membrane

### **Nomenclature**

$A_m$	Surface membrane area [ $\text{dm}^2$ ]
$C_{\text{Cu}^{2+},d}$	Salt diffusate concentration [M]
$C_{\text{Cu}^{2+},r}$	Salt retentate concentration [M]
$\text{Cu}^{2+}$ rejection	Copper rejection [%]
$C_{i,d}$	Bulk diffusate concentration of i-component [M]
$C_{i,r}$	Bulk retentate concentration of i-component [M]
DD	Diffusion Dialysis
$F_d$	Volumetric diffusate flowrate $\left[\frac{\text{L}}{\text{s}}\right]$
$F_r$	Volumetric diffusate flowrate $\left[\frac{\text{L}}{\text{s}}\right]$
$\text{H}_2\text{SO}_4$ Recovery	Acid Recovery Ratio [%]
$\text{H}_2\text{SO}_4$ Recovery, max	Maximum Acid Recovery Ratio [%]
$i$	Coefficient of Van't Hoff
$J_i$	Flux of the i-component $\left[\frac{\text{mol}}{\text{dm}^2 \cdot \text{s}}\right]$
$J_{dr}$	Drag flux $\left[\frac{\text{L}}{\text{h} \cdot \text{m}^2}\right]$
$J_{os}$	Osmotic flux $\left[\frac{\text{L}}{\text{h} \cdot \text{m}^2}\right]$
$k_{i,r}$	Mass retentate transport coefficient for the i-component $\left[\frac{\text{dm}}{\text{s}}\right]$
$k_{i,d}$	Mass diffusate transport coefficient for the i-component $\left[\frac{\text{dm}}{\text{s}}\right]$
$m_i$	Molality of the i-component $\left[\frac{\text{mol}}{\text{L solvent}}\right]$
$M_s$	Solvent molecular weight $\left[\frac{\text{g}}{\text{mol}}\right]$
$P_i$	Permeability of the membrane for the i-component $\left[\frac{\text{dm}}{\text{s}}\right]$
PS	Polystyrene
PSU	Polysulfone
$P_w$	Water permeability $\left[\frac{\text{L}}{\text{bar} \cdot \text{dm}^2 \cdot \text{s}}\right]$
R	Universal constant of ideal gases $\left[\frac{\text{J}}{\text{mol} \cdot \text{K}}\right]$
T	Temperature [ $^{\circ}\text{C}$ ]
$U_i$	Overall mass transfer coefficient of the i-component $\left[\frac{\text{dm}}{\text{s}}\right]$
$U_{\text{H}_2\text{SO}_4}$	Secondary overall mass transfer coefficient related to the presence of copper salts $\left[\frac{\text{dm}}{\text{s}}\right]$
$V_d$	Diffusate volume [L]
$V_{r,0}$	Initial retentate volume [L]
$V_s$	Solvent molar volume $\left[\frac{\text{m}^3}{\text{mol}}\right]$
$Z_{ch}$	Module length [dm]

### Greek letters

$\beta_i$	Hydration number of the specie i
$\Phi$	Osmotic coefficient
$\eta_{\text{H}_2\text{SO}_4}$	$\text{H}_2\text{SO}_4$ recovery efficiency [%]
$\pi_{r/d}$	Retentate/diffusate osmotic pressure [bar]

## References

- [1] A. Agrawal, K. K. Sahu, An overview of the recovery of acid from spent acidic solutions from steel and electroplating industries, *Journal of Hazardous Materials* 171 (2009) 61-75. <https://doi.org/10.1016/j.jhazmat.2009.06.099>.
- [2] C. Negro, M. A. Blanco, F. López-Mateos, A. M. C. P. DeJong, C. LaCalle, J. Van Erkel, D. Schmal, Free acids and chemicals recovery from stainless Steel pickling baths, *Separation Science and Technology* 36 (2001) 1543-1556. <https://doi.org/10.1081/SS-100103887>.
- [3] G. Leonzio, Recovery of metal sulphates and hydrochloric acid from spent pickling liquors, *Journal of Cleaner Production* 129 (2016), 417-426. <https://doi.org/10.1016/j.jclepro.2016.04.037>.
- [4] J. Luo, C. Wu, T. Xu, Y. Wu, Diffusion dialysis-concept, principle and applications, *Journal of Membrane Science* 366 (2011) 1-16. <https://doi.org/10.1016/j.memsci.2010.10.028>.
- [5] J. Ran, L. Wu, Y. Ru, M. Hu, L. Din, T. Xu, Anion exchange membranes (AEMs) based on Poly (2,6-dimethyl-1,4-phenylene oxide) (PPO) and its derivatives, *Polymer Chemistry* 6 (2015) 5809-5826. <https://doi.org/10.1039/c4py01671h>.
- [6] M. I. Khan, A. N. Mondal, C. Cheng, J. Pan, K. Emmanuel, L. Wu, T. Xu, Porous BPPO-based membranes modified by aromatic amine for acid recovery, *Separation and Purification Technology* 157 (2016) 27-34. <https://doi.org/10.1016/j.seppur.2015.11.028>.
- [7] J. Jeong, M. S. Kim, B. S. Kim, S. K. Kim, W. B. Kim, J. C. Lee, Recovery of H<sub>2</sub>SO<sub>4</sub> from waste acid solution by a diffusion dialysis method, *Journal of Hazardous Materials B124* (2005) 230-235. <https://doi.org/10.1016/j.jhazmat.2005.05.005>.
- [8] S. H. Lin, M. C. Lo, Recovery of sulfuric acid from waste aluminium surface processing solution by diffusion dialysis, *Journal of Hazardous Material* 60 (1998) 247-257. [https://doi.org/10.1016/S0304-3894\(98\)00099-5](https://doi.org/10.1016/S0304-3894(98)00099-5).

- [9] Z. Palatý, A. Záková, Transport of sulfuric acid through anion-exchange membrane NEOSEPTA-AFN, *Journal of Membrane Science* 119 (1996) 183-190. [https://doi.org/10.1016/0376-7388\(96\)00122-6](https://doi.org/10.1016/0376-7388(96)00122-6).
- [10] H. Bendová, Z. Palatý, Modeling of continuous diffusion dialysis of aqueous solutions of sulphuric acid and nickel sulphate, *Membrane Water Treatment* 2 (2011) 267-279. <https://doi.org/10.12989/mwt.2011.2.4.267>.
- [11] J. Xu, D. Fu, S. Lu, The recovery of sulphuric acid from the waste anodic aluminium oxidation solution by diffusion dialysis, *Separation and Purification Technology* 69 (2009) 168-173. <https://doi.org/10.1016/j.seppur.2009.07.015>.
- [12] K. Wang, Y. Zhang, J. Huang, T. Liu, J. Wang, Recovery of sulfuric acid from a stone coal acid leaching solution by diffusion dialysis, *Hydrometallurgy* 173 (2017) 9-14. <https://doi.org/10.1016/j.jhazmat.2009.11.017>.
- [13] Z. Palatý, H. Bendová, Permeability of a Fumasep FAD membrane for selected inorganic acids, *Chemical Engineering & Technology* 41 (2017) 385-391. <https://doi.org/10.1002/ceat.201700595>.
- [14] Z. Palatý, A. Záková, Diffusion dialysis of sulfuric acid in a batch cell, *Collection of Czechoslovak Chemical Communications* 59 (1994) 1971-1982. <https://doi.org/10.1135/cccc19941971>.
- [15] Z. Palatý, A. Záková, Apparent diffusivity of some inorganic acids in anion-exchange membrane, *Journal of Membrane Science* 173 (2000) 211-223. [https://doi.org/10.1016/S0376-7388\(00\)00363-X](https://doi.org/10.1016/S0376-7388(00)00363-X).
- [16] Z. Palatý, A. Záková, Transport of some strong incompletely dissociated acids through anion-exchange membrane, *Journal of Colloid and Interface Science* 268 (2003) 188-199. <https://doi.org/10.1016/j.jcis.2003.07.034>.



- [17] M. Ersoz, I. H. Gugul, A. Sahin, Transport of acids through polyether-sulfone anion exchange membrane, *Journal of Colloid and Interface Science* 237 (2001) 130-135.  
<https://doi.org/10.1006/jcis.2001.7487>.
- [18] D. H. Kim, J. H. Park, S. J. Seo, J. S. Park, S. Jung, Y. S. Kang, J. H. Choi, M. S. Kamg, Development of thin anion-exchange pore-filled membranes for high diffusion dialysis performance, *Journal of Membrane Science* 447 (2013) 80-86. <https://doi.org/10.1016/j.memsci.2013.07.017>.
- [19] J. Luo, C. Wu, Y. Wu, T. Xu, Diffusion dialysis processes of inorganic acids and their salts: the permeability of different acidic anions, *Separation and Purification Technology* 78 (2011) 97-102. <https://doi.org/10.1016/j.seppur.2011.01.028> [Get rights and content](#).
- [20] X. Tongwen, Y. Weihua, Sulfuric acid recovery from titanium white (pigment) waste liquor using diffusion dialysis with a new series of anion exchange membranes-static runs, *Journal of membrane* 183 (2001) 193-200. [https://doi.org/10.1016/S0376-7388\(00\)00590-1](https://doi.org/10.1016/S0376-7388(00)00590-1).
- [21] W. L. Wang, Y. Zhang, J. Huang, X. Zhu, Y. Wang, Separation and recovery of sulfuric acid from acidic vanadium leaching solution by diffusion dialysis, *Separation and Purification Technology* 96 (2012) 44-49. <https://doi.org/10.1016/j.seppur.2012.05.011>.
- [22] Z. Palatý, A. Záková, Separation of  $\text{H}_2\text{SO}_4 + \text{CuSO}_4$  mixture by diffusion dialysis, *Journal of Hazardous Materials* 114 (2004) 69-74. <https://doi.org/10.1016/j.jhazmat.2004.06.023>.
- [23] Ch. Amrane, K. E. Bouhidel, Integrated diffusion dialysis precipitation-cementation for selective recovery of leaching chemicals and metal values from electroplating sludge, *Hydrometallurgy* 177 (2018) 34-40. <https://doi.org/10.1016/j.hydromet.2018.02.011>.
- [24] S. K. Oh, S. H. Moon, T. Davis, Effects of metal ions on diffusion dialysis of inorganic acids, *Journal of Membrane Science* 169 (2000) 95-105. [https://doi.org/10.1016/S0376-7388\(99\)00333-6](https://doi.org/10.1016/S0376-7388(99)00333-6).
- [25] H. Bendová, Z. Palatý. Continuous separation of an  $\text{H}_2\text{SO}_4/\text{CuSO}_4$  mixture by diffusion dialysis, *Chemical Engineering Technology* 34 (2011) 217-224. <https://doi.org/10.1002/ceat.201000381>.

- [26] M. Janiszewska, A. Arguillarena, M. Wajs, K. Staszak, M. Regel-Rosocka, Application of diffusion dialysis for reduction of acidity of real pregnant leach solutions containing Ni and Co ions, *Separation Science and Technology*, 2019. <https://doi.org/10.1080/01496395.2019.1634102>.
- [27] <http://www.rewacem.eu/profile/>.
- [28] R. Gueccia, S. Randazzo, D. Chillura Martino, A. Cipollina, G. Micale, Experimental investigation and modelling of diffusion dialysis for HCl recovery from waste pickling solution. *Journal of Environmental Management* 235 (2019) 202-212. <https://doi.org/10.1016/j.jenvman.2019.01.028>.
- [29] M. Laliberté, W. E. Cooper, Model for Calculating the Density of Aqueous Electrolyte Solutions, *Journal of Chemical and Engineering Data* 49 (2004) 1141-1151. <https://doi.org/10.1021/je0498659>.
- [30] D. Van Gauwbergen, J. Baeyens, C. Creemers, Modelling osmotic pressures for aqueous solutions for 2-1 and 2-2 electrolytes, *Desalination* 109 (1997) 57-65. [https://doi.org/10.1016/S0011-9164\(97\)00056-8](https://doi.org/10.1016/S0011-9164(97)00056-8).
- [31] K. S. Pitzer, R. N. Roy, L. F. Silvester, Thermodynamics of Electrolytes: 7. Sulfuric Acid, *Journal of the American Chemical Society* 99 (1977) 4930-4936. <https://doi.org/10.1021/ja00457a008>.
- [32] J. M. Casas, F. Alvarez, L. Cifuentes, Aqueous speciation of sulfuric acid-cupric sulfate solutions, *Chemical Engineering Science* 55 (2000) 6223-6234. [https://doi.org/10.1016/S0009-2509\(00\)00421-8](https://doi.org/10.1016/S0009-2509(00)00421-8).
- [33] N. D. Nikolic, Lj. J. Pavlovic, S. B. Krstic, M. G. Pavlovic, K. J. Popov, Influence of ionic equilibrium in the  $\text{CuSO}_4\text{-H}_2\text{SO}_4\text{-H}_2\text{O}$  system on the formation of irregular electrodeposits of copper, *Chemical Engineering Science* 63 (2008) 2824-2828. <https://doi.org/10.1016/j.ces.2008.02.022>.
- [34] V. Vchirawongkwin, B. M. Rode, I. Persson, Structure and Dynamics of sulfate Ion in Aqueous Solution-An *ab initio* QMCF MD Simulation and Large Angle X-ray Scattering Study, *The Journal of Physical Chemistry B* 111 (2007) 4150-4155. <https://doi.org/10.1021/jp0702402>.

- [35] Ch. Akilan, G. Hefter, N. Rohman, R. Buchner, Ion Association and Hydration in Aqueous Solutions of Copper (II) Sulfate from 5 to 65 °C by Dielectric Spectroscopy, *The Journal of Physical Chemistry B* 110 (2006) 14961-14970. <https://doi.org/10.1021/jp0620769>.
- [36] J. Y. Xiang, J. W. Ponder, An Angular Overlap Model for Cu (II) Ion in the AMOEBA Polarizable Force Field, *Journal of Chemical Theory and Computation* 10 (2014) 298-311. <https://doi.org/10.1021/ct400778h>.
- [37] V. S. Bryantsev, M. S. Diallo, A. C. T. van Duin, W. A. Goddard III, Hydration of copper (II): New Insights from Density Functional Theory and the COSMO Solvation Model, *The Journal of Physical Chemistry A* 112 (2008) 9104-9112. <https://doi.org/10.1021/jp804373p>.
- [38] <http://www.astom-corp.jp/en/product/10.html>.
- [39] C. Wei, X. Li, Z. Deng, G. Fan, M. Li, C. Li, Recovery of H<sub>2</sub>SO<sub>4</sub> from an acid leach solution by diffusion dialysis, *Journal of Hazardous Materials* 176 (2010) 226-230. <https://doi.org/10.1016/j.jhazmat.2009.11.017>.
- [40] Z. Palatý, H. Bendová, Batch dialysis of phosphoric acid. Quantification of acid and water transport through Fumasep FAD membrane, *Separation and Purification Technology* 212 (2019) 605-610. <https://doi.org/10.1016/j.seppur.2018.11.076>.